

Many faces of low mass neutralino dark matter in the unconstrained MSSM, LHC data and new signals

Arghya Choudhury¹ and Amitava Datta²

*Indian Institute of Science Education and Research - Kolkata,
Mohanpur Campus, PO: BCKV Campus Main Office,
Nadia, West Bengal - 741252, India.*

Abstract

If all strongly interacting sparticles (the squarks and the gluinos) in an unconstrained minimal supersymmetric standard model (MSSM) are heavier than the corresponding mass lower limits in the minimal supergravity (mSUGRA) model, obtained by the current LHC experiments, then the existing data allow a variety of electroweak (EW) sectors with light sparticles yielding dark matter (DM) relic density allowed by the WMAP data. Some of the sparticles may lie just above the existing lower bounds from LEP and lead to many novel DM producing mechanisms not common in mSUGRA. This is illustrated by revisiting the above squark-gluino mass limits obtained by the ATLAS Collaboration, with an unconstrained EW sector with masses not correlated with the strong sector. Using their selection criteria and the corresponding cross section limits, we find at the generator level using Pythia, that the changes in the mass limits, if any, are by at most 10-12 % in most scenarios. In some cases, however, the relaxation of the gluino mass limits are larger ($\approx 20\%$). If a subset of the strongly interacting sparticles in an unconstrained MSSM are within the reach of the LHC, then signals sensitive to the EW sector may be obtained. This is illustrated by simulating the $blj E_T$, $l = e$ and μ , and $b\tau j E_T$ signals in i) the light stop scenario and ii) the light stop-gluino scenario with various light EW sectors allowed by the WMAP data. Some of the more general models may be realized with non-universal scalar and gaugino masses.

¹arghyac@iiserkol.ac.in

²adatta@iiserkol.ac.in

1 Introduction

The ATLAS and the CMS collaborations have been searching for supersymmetry (SUSY) [1] at the ongoing LHC 7 TeV experiments [2, 3, 4, 5]. No signal has been seen so far. A number of phenomenological analyses of the prospect of susy search at 7 TeV have also been published [6].

The recently announced results for $1 fb^{-1}$ data [2, 3, 4, 5] have been presented as constraints in the popular minimal supergravity (mSUGRA) model [7]³. As expected the jets + \cancel{E}_T channel, which arises from squark-gluino pair production in all combinations with large cross sections and is not suppressed due to small branching ratios, yields the strongest constraints on squark-gluino masses.

However, due to the special correlations among the superparticle (sparticle) masses in mSUGRA, the above mass bounds on strongly interacting sparticles impose stringent indirect lower bounds on the sparticle masses in the electroweak (EW) sector consisting of the sleptons and the electroweak gauginos. In many cases these model dependent bounds are significantly stronger than the corresponding direct bounds from LEP [8]. On the other hand, as we shall elaborate below by revising the existing limits, for any choice of squark-gluino masses compatible with the jets + \cancel{E}_T data there may exist a variety of EW sectors with much lighter sparticles compared to that in mSUGRA. In fact the jets + \cancel{E}_T data is only mildly sensitive to the electroweak sector in most cases (some exceptions will be listed below). Thus it is desirable to think of signals at the LHC which are directly sensitive to the electroweak sector.

One of the main attractive features of R-parity conserving SUSY is that the lightest supersymmetric particle (LSP) is stable. In many models the weakly interacting lightest neutralino ($\tilde{\chi}_1^0$) is assumed to be the LSP and it turns out to be a very popular candidate for the observed dark matter (DM) in the universe [9, 10]. The observed dark matter (DM) relic density (Ωh^2) in the universe has been precisely measured by the Wilkinson Microwave Anisotropy Probe (WMAP) collaboration [11] and if 10% theoretical uncertainty is added [12] then DM relic density is bounded by $0.09 \leq \Omega h^2 \leq 0.13$ at 2σ level. EW sectors with relatively low mass sparticles can provide many DM producing mechanisms yielding relic densities consistent with the data. As mentioned in the last paragraph such possibilities are

³The model we consider is also referred to as the constrained minimal supersymmetric standard model (CMSSM) in the literature.

now mostly excluded in the mSUGRA framework by the LHC experiments. The negative impact of early LHC data on low mass neutralino DM and on the prospect of direct DM search experiments were noted in [13]. However, this exclusion based on strongly model dependent assumptions is certainly not the final verdict on neutralino DM since the SUSY breaking mechanism is essentially unknown. Hence it is worthwhile to revisit the viable DM producing mechanisms within frameworks more general than mSUGRA invoking as little model dependent assumptions as is practicable.

It has recently been emphasized [14] that there are many relic density producing mechanisms involving light electroweak sectors, which are practically independent of the strong sector leaving aside the possibility of the coannihilation of the LSP with the lighter top squark (\tilde{t}_1) [15]. Thus any model with all strongly interacting sparticles beyond the reach of the LHC - 7 TeV experiments and a relatively light electroweak sector consistent with the observed relic density is allowed by the LHC data. In [14] no model dependent correlation among the sparticle masses in the strong and EW sectors was imposed. However, for the sake of simplicity it was assumed that the masses in the EW sector are correlated as in mSUGRA. Several observable signals involving parameter spaces consistent with both LHC and WMAP data were proposed. In this paper we give up the last assumption and study the impact of light EW sectors in an unconstrained minimal supersymmetric extension of the standard model (MSSM) on both LHC signals and the relic density data.

Obviously the best way to test such models would be signals at a new $e^+ - e^-$ collider directly sensitive to only EW sparticles with masses \gtrsim the corresponding lower limits from LEP. In the absence of such an accelerator one can look, e.g., for the clean 3l ($l = e$ or μ) signal from Chargino-neutralino pair production [16] and di-lepton + \cancel{E}_T signal from slepton pair production [17]. Apriority both the signals are viable even if the strongly interacting sparticles are heavy.

The experience from the simulations of the LHC-14 TeV experiments [18], however, does not encourage optimistic expectation at the on going experiments. In the former case chargino-neutralino masses modestly above the LEP limits were found to be observable. One can improve the chargino-neutralino mass reach to some extent by considering 2l + 1 τ and 1l + 2 τ events along with the 3l events [19]. It is also estimated that sleptons with masses \lesssim 400 GeV can be probed at the LHC-14 TeV with $\mathcal{L} \gtrsim 30 \text{ fb}^{-1}$ (see [18]).

Models in which only a sub-set of the strongly interacting sparticles along with light EW

sparticles are within the reach of the current LHC experiment are also compatible with the data. The decay of the strongly interacting sparticles into final states involving EW sparticles may provide new signals of reasonable size. Some examples illustrating this [3, 14, 20] have already been discussed. However, the analyses in [14, 20] were done when either the 1 fb⁻¹ data were not available or available in the unpublished form without many details. In this paper we shall improve these analyses using the published data and more general EW sectors consistent with the WMAP data as elaborated above. Our main goals are to check the impact of the more general models on i) the squark-gluino mass limits already obtained within the framework of mSUGRA and ii) the viability of the signals proposed in [14, 20] for more general scenarios.

In the simplest scenario considered in this paper following [14, 20], the lighter stop squark \tilde{t}_1 is assumed to be the only strongly interacting sparticle accessible to the current LHC experiments. Other groups have also investigated the light \tilde{t}_1 scenarios [22, 23]. If this squark is the next lightest supersymmetric particle (NLSP), then it will decay via the loop induced final state consisting of a charm quark and the LSP. As noted earlier the DM relic density may be produced in such a scenario via \tilde{t}_1 -LSP coannihilation. This channel has been investigated recently but does not appear to be very promising [24, 25]. Recently novel signals of \tilde{t}_1 NLSP have been proposed [26, 27]. However, the competition between the above mode and the four body decay of the \tilde{t}_1 NLSP [28] may further complicate the issue. The consequences of this competition in the context of the Tevatron experiments have already been discussed [29].

It was recently pointed out in ref [14, 20] that if this squark decays dominantly into the lighter chargino ($\tilde{\chi}^\pm$) and a b-quark, then viable signals sensitive to the EW sector may appear in the $blj \cancel{E}_T$ and $b\tau j \cancel{E}_T$ channels. However, for \tilde{t}_1 within the reach of the ongoing LHC experiments the above signals cannot survive the strong cuts on \cancel{E}_T and M_{eff} usually employed for general squark-gluino searches in jets + \cancel{E}_T by the LHC collaborations. Softer dedicated cuts need to be employed for this signal as shown in [14, 20]. In this paper we shall revisit the signals for more general EW sectors as elaborated above.

Another class of models interesting in the context of the LHC experiments are the ones with both the \tilde{t}_1 and the gluinos are within the reach of the current experiments: the light stop-gluino (LSG) model [14, 23]. This scenario can be realized in models with non-universal scalar and gaugino masses at the GUT scale [14]. The same signals as discussed

in the last paragraph may arise in this case also via the production of gluino pairs which then decay dominantly into $t\tilde{t}_1$ pairs. It may be recalled that the ATLAS collaboration has already investigated the $blj\cancel{E}_T$ signal [3]. However, the hard cuts proposed for separating the background eliminates the events from the direct \tilde{t}_1 pair production. As a result the gluino mass limit (500-520 GeV) obtained by them is by and large independent of the $m_{\tilde{\tau}}$. On the other hand the alternative selection criteria with softer cuts as proposed in [14, 20] can separate the $blj\cancel{E}_T$ events from \tilde{t}_1 pair production from the ones coming from gluino pair production. In this paper we shall follow this approach and shall revisit the signal for the more general EW sectors discussed above. Moreover the complementary channel $b\tau j\cancel{E}_T$ which is more important when the electroweak gauginos decay dominantly in τ -rich final states was not considered in [3]. This signal was studied for the first time in [14].

The plan of the paper is as follows. Section 2 contains all the results obtained in this paper and the related discussions. In Section 2.1 we list the input parameters for the unconstrained EW sector. The main departures from the mSUGRA spectrum are duly emphasized. The possibility of accommodating these departures with non-universal scalar and gaugino masses are discussed as and when appropriate. In sub-section 2.2 the parameter space in the unconstrained EW sector consistent with WMAP data is delineated. DM relic density producing mechanisms which are not allowed in mSUGRA but occur frequently in more general scenario are pointed out. Revision of the squark-gluino mass bounds in mSUGRA for more general EW sectors consistent with WMAP data is presented in the sub-section 2.3. Novel signal in the $blj\cancel{E}_T$ and $b\tau j\cancel{E}_T$ channels in the light stop and LSG scenarios are also included in this section. Our conclusions will be summarized in Section 3.

2 Results and Discussions :

2.1 Models and Parameters :

The popular mSUGRA model [7] has only five free parameters including soft SUSY breaking terms. These are m_0 (the common scalar mass), $m_{1/2}$ (the common gaugino mass), A_0 (the common trilinear coupling), all given at the gauge coupling unification scale ($M_G \sim 2 \times 10^{16}$ GeV); the ratio of the Higgs vacuum expectation values at the electroweak scale namely $\tan\beta$ and the sign of μ . The magnitude of μ is determined by the radiative electroweak symmetry

breaking condition.

In contrast in the phenomenological MSSM M_1, M_2, M_3 are the three gaugino mass parameters at the weak scale and no special relation among them is assumed. It is known for a long time that even in mGUGRA type models where masses at the weak scale are determined by some boundary conditions at a high scale, a variety of gaugino mass relations at the weak scale may emerge due to non-universal boundary conditions for gaugino masses at M_G [30].

We also consider the following weak scale parameters. $M_{\tilde{q}_i}$ is the mass parameter for the i th ($i = 1, 2$ and 3 is the generation index) generation squarks of the L-type belonging to a doublet of $SU(2)_L$. $M_{\tilde{u}_i}$ ($M_{\tilde{d}_i}$) is the mass parameter for the R-type singlet up (down) squarks. Similarly $M_{\tilde{l}_i}$ ($M_{\tilde{\tau}_i}$) is the left (right) type slepton mass parameter for the i th generation. A_t, A_b, A_τ are the 3rd generation trilinear soft couplings. The other input parameters are the mass of pseudoscalar Higgs boson m_A , the higgsino mixing parameter μ and $\tan\beta$.

In our numerical analysis we have assumed that all squarks and gluinos are beyond the reach of the LHC 7 TeV run ⁴. For the sake of simplicity we have taken $M_{\tilde{q}_1} = M_{\tilde{q}_2} = M_{\tilde{q}_3} = M_{\tilde{u}_1} = M_{\tilde{u}_2} = M_{\tilde{u}_3} = M_{\tilde{d}_1} = M_{\tilde{d}_2} = M_{\tilde{d}_3} = 1.5$ TeV. For the relic density computation in this subsection we also take M_3 (which defines the gluino mass) = 1.5 TeV at the weak scale.

We have further assumed that $M_{\tilde{l}_1} = M_{\tilde{l}_2} = M_{\tilde{\tau}_1} = M_{\tilde{\tau}_2} = M_{\tilde{l}} ; M_{\tilde{l}_3} = M_{\tilde{\tau}_3}$; but these common masses at the weak scale are treated as free parameters. The equality of the slepton mass parameters at the weak scale is not realized in mSUGRA, where L-type sleptons are typically heavier than the R-type. Since the sneutrino mass is correlated with that of L-type sleptons, it also exceed R- type slepton masses over most of the parameter space. On the other hand models with non-universal scalar masses at the high scale can yield considerably different mass hierarchies among the two types of sleptons at the weak scale. The running of the common scalar masses at the SUSY breaking scale (say, the Planck scale) to the GUT scale (M_G) may create the above nonuniversality when L and R type sleptons belong to different representations of the GUT group [31]. When a GUT group breaks down to a group of lower rank, certain $U(1)$ symmetry breaking D-terms can also lead to such non-universality [32].

⁴All masses and parameters having the dimension of mass are in GeV unless stated otherwise.

Relatively light sleptons and, consequently, sneutrinos can affect the DM relic density production through LSP annihilation via slepton exchange and / or via LSP-sneutrino co-annihilation in a large region of the parameter space where the sneutrino happens to be the next lightest supersymmetric particle (NLSP). In the context of collider phenomenology, the relative probabilities of m -lepton + n -jet + E_T signatures, for different m and n , may turn out to be quite distinct in comparison to mSUGRA [33] in such models. This may distinguish between different models.

In addition we assume $A_t = A_b = A_\tau = -600$; $\mu = 362.0$; $m_A = 1$ TeV and $\tan\beta = 10$. Moreover since our focus is on a light EW sector the mass parameters in this sector are restricted - somewhat arbitrarily - to be less than 200. As a result we have either a bino dominated LSP or an admixture of bino and wino with negligible Higgsino component.

In this parameter space the computed mass of the lighter Higgs scalar (m_h), after taking into account a theoretical uncertainty of 3 [34], satisfies the LEP bound $m_h \geq 114.4$ [35]. Further discussion of m_h in the light of more recent experiments is given below.

We have used micrOMEGAs (v.2.4.1) [36] for computing the DM relic density. The susy particles spectra and the decay branching ratios (BRs) have been computed by SUSPECT [37] and SDECAY [38].

In Fig. 1 we plot Ωh^2 vs M_1 for different choices of the other parameters in the EW sector. We have also checked that varying the $m_{\tilde{\tau}_1}$ or $m_{\tilde{g}}$ does not affect the DM relic density, unless the difference between $m_{\tilde{\tau}_1}$ and $m_{\tilde{\chi}_1^0}$ is so small that the possibility of stop-neutralino coannihilation [15] opens up.

To begin with we have searched for the parameter space allowed by the WMAP data. Results are given in Fig. 1. Here we have plotted Ωh^2 vs M_1 for different M_2 and common slepton masses. We have chosen the following five representative sets of M_2 and the common slepton mass of the third generation ($M_{\tilde{l}_3} = M_{\tilde{\tau}_3}$): model-1 (110,115), model-2 (110,150) , model-3 (150,115), model-4 (150,200) and model-5 (200,200). The choices $M_2 = 110, 150$ and 200 yield $m_{\tilde{\chi}_\pm} = 106, 145$ and 191 respectively while $M_{\tilde{l}_3} = M_{\tilde{\tau}_3} = 115, 150$ and 200 result in $m_{\tilde{\tau}_1} = 89, 131, 186$ respectively. For each combination of M_2 and $M_{\tilde{\tau}_3}$, we have varied the common slepton mass ($M_{\tilde{l}_i}$) for the first two generations in steps of 10 in the range 100 to 200. Thus we allow the lighter $\tilde{\tau}$ mass eigenstate ($\tilde{\tau}_1$) to be lighter or heavier than the sleptons belonging to the first two generations. This is also a significant departure from the mSUGRA spectrum. It should be noted that we have several choices where the masses

of the sparticles in the electroweak sector are just above the corresponding LEP limits.

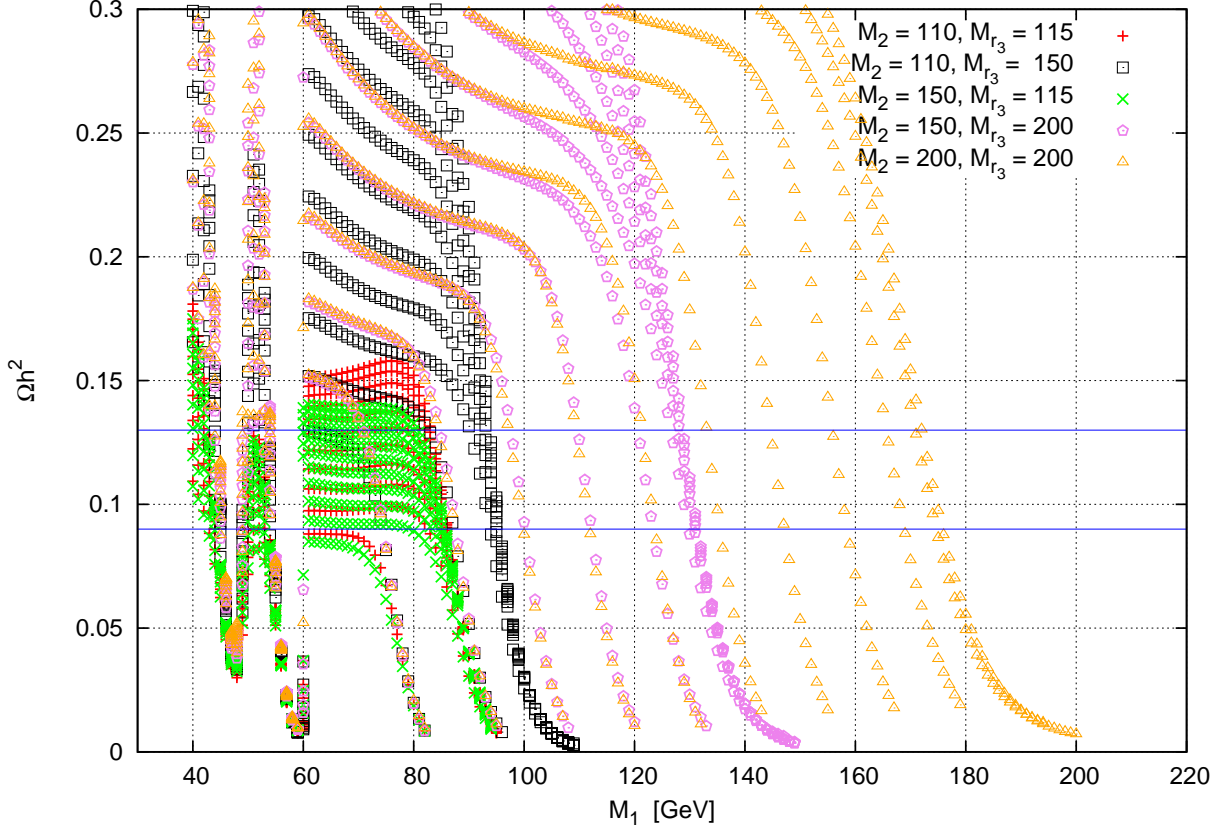


Figure 1: M_1 vs Ωh^2 for different choices of M_2 , $M_{\tilde{r}_3}$ ($= M_{\tilde{l}_3}$) and $M_{\tilde{l}}$ ($= M_{\tilde{l}_1} = M_{\tilde{l}_2} = M_{\tilde{r}_1} = M_{\tilde{r}_2}$). Blue horizontal lines represent the WMAP allowed DM relic density band (0.09 to 0.13).

In Fig 1, each color or point shape corresponds to a particular choice of M_2 and $M_{\tilde{r}_3}$ as indicated in the upper right corner. The ten different lines of the same color or type in Fig. 1 correspond to different choice of $M_{\tilde{l}}$.

Throughout this work the pole mass of the top quark (running bottom quark mass evaluated in the \overline{MS} scheme) will be taken as m_t (m_b) = 173.2 (4.25). We have also included the current constraints on squarks, sleptons, gluino, chargino, neutralinos and the lighter scalar Higgs boson masses obtained from collider data. For example in the CMSSM models with $\tan\beta = 10$, $A_0 = 0$ and $\mu > 0$, ATLAS has excluded squarks and gluinos having

equal mass below 950 GeV [2]. We shall assume that $m_{\tilde{\chi}^\pm} \geq 103.5$, all the sleptons (except the lighter stau mass eigenstate) are heavier than 100. This is basically a simplified form of the LEP limits. The lighter $\tilde{\tau}$ mass eigenstate is assumed to be heavier than 86 as required by the LEP data. We emphasize that there is no model independent bound on $m_{\tilde{\chi}_1^0}$ from collider data. From the chargino mass bound from LEP there is a bound $m_{\tilde{\chi}_1^0} > 50.8$ for $\tan\beta = 10$ and $\mu > 0$, which is valid in mSUGRA. From LHC, WMAP and XENON100 [39] there is a bound $m_{\tilde{\chi}_1^0} \geq 160$ in mSUGRA [40]. We have only considered parameter spaces resulting in 114.4 [35] $< m_h < 127$ [41, 42]. We have checked that recent hint of a peak at $m_h \approx 125$ reported by the LHC collaborations [41], which is not yet statistically significant, can be accommodated if we make A_0 large (say 1.5 TeV). However, our parameter space allowed by the relic density data is not drastically affected by the choice of A_0 . The impact of the m_h bound on different SUSY models and various observables has been considered by several groups [43].

2.2 Summary of Fig.1 :

There are five sets of data :

- **Model- 1** : The red points (marked by +) represent the computed Ωh^2 in this parameter space. Here both $\tilde{\chi}_1^\pm$ and $\tilde{\tau}_1$ lie just above the LEP limit. The latter is the NLSP for the entire parameter space scanned and its mass sets the limit for the LSP mass.
- **Model-2** : The squares represent the computed relic density. Here the mass of the $\tilde{\chi}_1^\pm$ is just above the LEP limit and it is the NLSP for the whole parameter space studied. The mass of $\tilde{\tau}_1$ is somewhat away from the LEP limit.
- **Model-3** : The green cross marks represent the parameter space with $M_2 = 150$, $M_{\tilde{\tau}_3} = 115$. Here the mass of $\tilde{\tau}_1$ is just above the LEP limit and it is the NLSP in our study. However, the mass of $\tilde{\chi}_1^\pm$ is away from the LEP limit.
- **Model-4** : Relic densities are represented by the violet pentagons. In this case both $\tilde{\chi}_1^\pm$ and $\tilde{\tau}_1$ have masses far away from the the LEP limit. For relatively low common slepton masses the sneutrino is the NLSP. Otherwise the chargino is the NLSP.

- **Model-5** : In this case the orange triangles represent the relic densities. Over most of the parameter space the sneutrino is the NLSP. For the highest common slepton mass (200), the lighter stau, the sneutrino and the chargino have closely spaced masses.

We have also demarcated the WMAP allowed DM relic density band (0.09 to 0.13) by the blue horizontal lines. In the next section we will take different benchmark points from this region for studying the impact of this more general EW sector on LHC physics.

The importance of LSP annihilation via relatively low mass R-type slepton exchange (Bulk annihilation) in producing the observed relic density is well known in mSUGRA [9, 10]. The corresponding region of the parameter space (the Bulk region) is, however, strongly disfavoured by the current LHC constraints as they do not permit the sleptons to be sufficiently light. In the unconstrained MSSM this mechanism retains its importance for certain ranges of the LSP mass where both L and R type slepton exchange may be important. However, even for smaller and larger LSP masses there are many other potentially important relic density producing mechanisms.

In order to streamline the discussions, we divide the whole region allowed by the WMAP data into three parts according to the value of M_1 as follows :

I) $40 \lesssim M_1 \lesssim 60$: In this region different choices of M_2 consistent with LEP data give almost the same DM relic density, which, however, depends strongly on the slepton masses. The neutralinos studied in this paper are either bino dominated or mixture of bino and wino. For such neutralinos, $m_{\tilde{\chi}_1^0}$ significantly smaller than 40 are not allowed due to the LEP lower bounds on chargino and slepton masses and the WMAP constraints. In fact we have checked that $m_{\tilde{\chi}_1^0} \gtrsim 35$ in the parameter space we have scanned.

Three main mechanisms or combinations operate in this case: i) bulk annihilation, ii) annihilation mediated by a Z boson of low virtuality or iii) mediated by the lighter Higgs scalar (h) of low virtuality. It should be noted that even if we ignore the indirect bound on $m_{\tilde{\chi}_1^0}$ from the LHC bounds in mSUGRA, a large part of this region is strongly disfavoured in mSUGRA due to the LSP mass bound from LEP inferred from the chargino mass limit. We also stress that no co-annihilation process can play any role in this parameter space due to the LEP lower bounds on EW sparticle masses.

For stau mass a little above the LEP bound (Model 1 or 3), $M_{\tilde{t}}$ not very far from the corresponding bound and the LSP mass below the Z resonance, this happens through pure bulk annihilation for a range of slepton masses (e.g., with $M_1 = 40$, $M_{\tilde{t}} < 130$). For higher

M_1 on both sides of the Z resonance, both bulk annihilation and annihilation via a virtual Z contributes adequately in all models. However, the slepton masses for which this happens is model dependent. For M_1 on the Z resonance or in its immediate vicinity the annihilation cross section is too large and Ωh^2 is too small for all LEP allowed slepton and stau masses.

Well above the Z resonance, the Z contribution begins to reduce. Now process iii) takes over. Combination of i) and iii) is now the potential mechanism. This happens in all models 1 - 5 but the range of $M_{\tilde{l}}$ is again model dependent. There is even a small parameter space where i), ii) and iii) all contributes significantly.

On the h resonance or in its immediate neighbourhood Ωh^2 is again too small. At $M_1 = 56$, Ωh^2 falls abruptly and nearly at $M_1 = 59$ we see a minima. This is due to the higgs resonance (here computed $m_h = 113 \pm 3$ (theoretical uncertainty)). Also here the relative contribution to $1/(\Omega h^2)$ is largest from the process $\tilde{\chi}_1^0 \tilde{\chi}_1^0 \rightarrow b \bar{b}$ (nearly 80 %).

II) $60 \lesssim M_1 \lesssim 80$: A large number of points in model 1 and 3, with $\tilde{\tau}_1$ NLSP, for different common slepton masses lie in the region allowed by WMAP data. The value of Ωh^2 remains almost constant for LSP masses in this range for fixed values of other parameters. Pure bulk annihilation is the source of DM relic density.

In models 2, 4 and 5 with heavier $\tilde{\tau}_1$, pure bulk annihilation is not viable. However, if the sneutrinos belonging to the first two generations are the NLSP, then a small but significant contribution from LSP- sneutrino coannihilation along with bulk annihilation may produce the required relic density. For each M_1 there is a narrow range of sneutrino masses where this happens. This mechanism is indicated by a sharp fall of the relic density over a narrow range of M_1 .

III) $80 \lesssim M_1 \lesssim 200$: In models 1 and 3, the LSP- $\tilde{\tau}_1$ coannihilation becomes effective for a small range of M_1 just above 80.

In models 2, 4 and 5 with heavier $\tilde{\tau}_1$, bulk annihilation alone can not produce the observed relic density. If the lighter chargino is the NLSP, several choices of the common slepton mass yield approximately the same relic density (see, e.g., the squares (model 2) in the neighbourhood of $M_1 \approx 95$). In fact Ωh^2 in this case primarily depends on the LSP and chargino properties alone. LSP annihilation into W pairs and LSP-Gaugino coannihilation are the significant mechanisms for relic density production. If, on the other hand, the sneutrino is the NLSP, then sneutrino co-annihilation and bulk annihilation may serve the purpose. This happens for a small range of the common slepton mass for each M_1 .

Several examples are shown in Fig. 1.

2.3 Collider Signals

In this section we discuss the collider signatures corresponding to some benchmark points allowed by both WMAP (see Section 2.2) and LHC data.

In this paper all leading order (LO) signal cross-sections have been computed by CalcHEP [44] unless otherwise stated. For any two body final state (except for QCD processes) with identical particles or sparticles both the renormalization and the factorization scales are taken as, $\mu_R = \mu_F = M$, where M is the mass of the particle or sparticle concerned ⁵. For two unequal masses in the final state the scales are taken to be the average of the two. For QCD events the scales have been chosen to be equal to $\sqrt{\hat{s}}$ which is the energy in the parton CM frame, and the cross-section is computed by Pythia [45]. All LO cross-sections are computed using CTEQ5L parton density functions (PDFs) [46].

The next to leading order (NLO) cross-sections for the signal processes have been computed by PROSPINO [48] using the CTEQ5M PDFs. The K-factors are computed by comparing with the LO cross-section. The LO cross-sections from PROSPINO agree well with CalcHEP for the same choice of the scales. The NLO cross sections are used to compute revised mass limits and the signal sizes presented in this section.

The NLO background cross-sections are not known for some backgrounds - in particular for the QCD processes. For computing the significance of the signal we conservatively multiply the total LO background by an overall factor of two.

We have considered the backgrounds from $t\bar{t}$, QCD events, $W + n\text{-jets}$ events and $Z + n\text{-jets}$, where W and Z decays into all channels. After the final cuts $t\bar{t}$, $W + 1j$ and $W + 2j$ are the main backgrounds. $t\bar{t}$ events are generated using Pythia and the LO cross-section has been taken from CalcHEP which is 85.5 pb. QCD processes are generated by Pythia in different \hat{p}_T bins : $25 \leq \hat{p}_T \leq 400$, $400 \leq \hat{p}_T \leq 1000$ and $1000 \leq \hat{p}_T \leq 2000$, where \hat{p}_T is defined in the rest frame of the parton collision. The main contribution comes from the low \hat{p}_T bin, which has a cross-section of $\sim 7.7E + 07$ pb. However, for the other two bins the background events are negligible.

For $W + n\text{-jets}$ events we have generated events with $n = 0, 1$ and 2 at the parton level

⁵See footnote 4.

using ALPGEN (v 2.13) [47]. We have generated these events subjected to the condition that $P_T^j > 20$, $\Delta R(j, j) \geq 0.3$ and $|\eta| \leq 4.5$. These partonic events have been fed to Pythia for parton showering, hadronization, fragmentation and decays etc.

We have used the toy calorimeter simulation (PYCELL) provided in Pythia with the settings described in [14, 20]. Lepton ($l = e, \mu$) selection, b -jet tagging and τ -jet identification are also implemented following these references.

The strongest limits on squark, gluino masses come from the jets + \cancel{E}_T channel. The ATLAS group has introduced five sets of selection criteria (SC) (see Table 1 of [2]) for new physics search in this channel. The observed number of events in this channel and the SM background estimated from the data for each of the above SC lead to a model independent upper bound on σ_{new} , the effective cross-sections for any new physics scenario. Five such bounds, thus obtained, are 22 fb, 25 fb, 429 fb, 27 fb and 17 fb respectively at 95% confidence level. These bounds can be used to obtain exclusion contours in any specific SUSY breaking model.

Some examples of the limits (L1-L4) obtained by the ATLAS collaboration in the mSUGRA/CMSSM model (See Fig. 2 (right) of [2]) for $\tan\beta = 10$, $A_0 = 0$ and $\mu > 0$ are given below.

L1) Squarks and gluinos of equal mass are excluded for masses below 950 GeV. Here the average squark mass is considered.

From the exclusion plot of ATLAS it also follows that $m_0 = 1.0$ (1.5) TeV and $m_{1/2} \sim 300$ (210) lies on the exclusion contour. It then follows that

L2) For average squarks mass of 1.1 TeV gluino masses below 780 GeV are excluded.

L3) For average squarks mass of 1.5 TeV gluino masses below 600 GeV are excluded.

For the validation our simulation, we focus on the above exclusion contour. By definition $\sigma_{new} = \sigma A \epsilon$, where σ is the raw production cross-section in any new physics scenario, A is the acceptance and ϵ is the efficiency [2]. We have chosen several points on this exclusion contour. For each point we compute A and ϵ corresponding to all the five SC of ATLAS from our simulation. For each mSUGRA point σ in the NLO is computed by PROSPINO. We find that each computed σ_{new} is reasonably close to at least one of the upper limits (see above) obtained by ATLAS. This reflects that our simulation in mSUGRA would lead to an exclusion contour pretty close to the one obtained by ATLAS. We follow this procedure to obtain new limits in other models.

We now turn our attention to more general models where the masses of the sparticles in the strong and EW sectors are assumed to be uncorrelated. We consider various EW sectors allowed by the WMAP data as illustrated in Fig. 1 of this paper and compute the squark-gluino mass limits from ATLAS bounds on σ_{new} .

Points	M_1	M_2	$M_{\tilde{t}}$	$M_{\tilde{t}_3}$	$m_{\tilde{\chi}_1^0}$	$m_{\tilde{\chi}_1^\pm}$	$m_{\tilde{\tau}_1}$	$m_{\tilde{L}}$
P1	45	150	160	200	43	145	186	166
P2	128	150	160	200	121	145	186	166
P3	43	150	200	115	40	145	89	205
P4	81	150	200	115	77	145	89	205
P5	45	110	150	150	42	106	131	157
P6	99	150	120	200	93	145	186	128
P7	94	110	200	150	88	106	131	205

Table 1: Parameters and mass spectra corresponding to different benchmark points taken from different regions of Fig. 1.

For a better understanding of the revised limits, we also select some benchmark EW sectors from Fig.1 (see Table 1). The corresponding BRs relevant for this discussion are presented in Table 2. Some important characteristics of the selected points are given below.

- The point P1 corresponds to a low $m_{\tilde{\chi}_1^0}$ not allowed by the LEP data in mSUGRA.
- For the point P2, the BR of the mode $\tilde{\chi}_1^\pm \rightarrow \tilde{\chi}_1^0 l \nu_l$, $l = e$ and μ , is large (78 %) compared to what is obtained over most of the mSUGRA parameter space. This is due to the fact that the decay $\tilde{\chi}_1^\pm \rightarrow \tilde{\chi}_1^0 W$ is not allowed and the common slepton mass is relatively low.
- For P3 and P4, the combined BR of the modes $\tilde{\chi}_1^\pm \rightarrow \tilde{\tau}_1 \nu_\tau$ and $\tilde{\nu}_\tau \tau$ is 100 %.
- In examples P5 and P7, $\tilde{\chi}_1^\pm$ is the NLSP. But the mass difference (Δm) between the $\tilde{\chi}_1^0$ and $\tilde{\chi}_1^\pm$ is large in P5 (65) and much smaller in P7 (19). The BR of the mode $\tilde{\chi}_1^\pm \rightarrow \tilde{\chi}_1^0 l \nu_l$ is 48 (23) % for the point P5 (P7).

- In P6, $\tilde{\nu}_\ell$ is the NLSP, $\tilde{\chi}_1^\pm$ is lighter than $\tilde{\tau}_1$ but heavier than \tilde{l}_L and $\tilde{\nu}_\ell$. Here BR of $\tilde{\chi}_1^\pm \rightarrow \tilde{\nu}_\ell l$ is 87% and $\tilde{\chi}_1^\pm \rightarrow \tilde{l}_L \nu_l$ is 13 %.

Decay Modes	P1	P2	P3	P4	P5	P6	P7
$\tilde{\chi}_1^\pm \rightarrow \tilde{\chi}_1^0 qq'$	-	17	-	-	30	-	51
$\rightarrow \tilde{\chi}_1^0 l \nu_l$	-	78	-	-	48	-	23
$\rightarrow \tilde{\chi}_1^0 \tau \nu_\tau$	-	5	-	-	22	-	26
$\rightarrow \tilde{\tau}_1 \nu_\tau$	-	-	36	36	-	-	-
$\rightarrow \tilde{\chi}_1^0 W$	100	-	-	-	-	-	-
$\rightarrow \tilde{\nu}_\tau \tau$	-	-	64	64	-	-	-
$\rightarrow \tilde{\nu}_\ell l$	-	-	-	-	-	87	-
$\rightarrow \tilde{l}_L \nu_l$	-	-	-	-	-	13	-
$\tilde{\tau}_1 \rightarrow \tilde{\chi}_1^0 \tau$	75	49	100	100	78	52	53
$\rightarrow \tilde{\chi}_2^0 \tau$	9	21	-	-	8	19	19
$\rightarrow \tilde{\chi}_1^\pm \nu_\tau$	16	30	-	-	14	29	28

Table 2: The BRs (%) of the dominant decay modes of $\tilde{\chi}_1^\pm$ and $\tilde{\tau}_1$ for the benchmark points.

In order to compare the new limits with the ones in mSUGRA, we fix the average squarks mass as in the examples L1, L2, L3 given above and vary $m_{\tilde{g}}$. We then compute the jets + E_T signature corresponding to EW sectors randomly chosen from the points in Fig. 1 allowed by WMAP data. If a gluino mass yields cross sections smaller than the ATLAS upper bounds on σ_{new} for all selection criteria, we reduce it keeping average squark mass fixed. In this way we obtain a relaxed limit on $m_{\tilde{g}}$ for a fixed average squark mass when the cross-section exceeds the upper bound on σ_{new} [2] for at least one selection criteria.

For most of the points considered by us, the $m_{\tilde{g}}$ limit changes at most by 10 to 12 % compared to the mSUGRA limit. For e.g., for the benchmark point P1 the lower bounds on $m_{\tilde{g}}$ in L1, L2, L3 are reduced by 50 to 70. As noted earlier this is due to relatively low $m_{\tilde{\chi}_1^0}$.

The leptonic BR of the $\tilde{\chi}_1^\pm$ is large for P6. The lepton veto in the ATLAS selection criteria relaxes the limits on $m_{\tilde{g}}$ in all cases by 70-80. This is reminiscent of the relaxation of the $m_{\tilde{q}} - m_{\tilde{g}}$ mass limits obtained from Tevatron data (see the 1st paper of [33]) for similar reasons.

On the other hand if $\text{BR}(\tilde{\chi}_1^\pm \rightarrow \tilde{\nu}_\tau \tau, \tilde{\tau}_1 \nu_\tau) = 100\%$ then the limit on $m_{\tilde{g}}$ is strengthened by 5-10 % due to the large BR of hadronic τ decays. The relative changes in the limits noted by us are typically of the order of the uncertainties in the production cross sections due to the choice of QCD scale and/or the parton density function. This simple exercise illustrates that ATLAS limits on squarks-gluino masses are approximately valid for many different electroweak sectors quite different from that in mSUGRA. However, we also arrive at the important conclusion that slepton and / or chargino masses just above the corresponding LEP limits are very much allowed by the current LHC data.

ATLAS CUTS [2] 'High Mass'	mSUGRA point with $m_0 = 2500, m_{1/2} = 185$ $A_0 = 0$ and $\tan\beta=10$	Benchmark point P1 with $m_{\tilde{g}} = 550$
P_T of leading jet ≥ 130	92 %	76 %
$\cancel{E}_T \geq 130$	54 %	33 %
P_T of 2nd jet ≥ 80	75 %	68 %
P_T of 3rd jet ≥ 80	79 %	78 %
P_T of 4th jet ≥ 80	57 %	61 %
$\cancel{E}_T/M_{eff} \geq 0.2$	47 %	32 %
$M_{eff} \geq 1100$	29 %	18 %

Table 3: Efficiency table for different cuts employed by ATLAS (see Table 1 of [2]) for deriving in mSUGRA the limit L4 (see text) and the corresponding efficiencies for the benchmark point P1.

L4) For heavy squarks (say 2.5 or 3.0 TeV) ATLAS data has excluded gluinos with masses in the range 550 to 570 .

Now keeping the average squarks mass as in L4 but choosing the EW sectors from Figure 1, we have checked the change in the limit on gluino mass. Some interesting examples are given below. Models with EW sector as in P1 significantly relax the limit on the gluino mass to 450. This is the largest relaxation of $m_{\tilde{g}}$ limit we have noted in this paper. In mSUGRA the limit L4 is obtained by the last cut set ('High Mass') employed by the ATLAS group [2]. The efficiencies for these cuts are presented in Table 3. For the same average squark mass and $m_{\tilde{g}}$, the corresponding efficiencies for the point P1 are displayed in Table 3 which are

found to be smaller in each case. Models with EW sectors as in P2 (P3) relaxes (strengthens) the gluino mass limit to 500 (620).

We next consider the light stop scenario (i.e., \tilde{t}_1 is the only strongly interacting sparticle within the reach of 7 TeV experiments) and examine the potential of the $blj \cancel{E}_T$ and $b\tau j \cancel{E}_T$ signals stemming from \tilde{t}_1 pair production for various EW sectors chosen from Fig 1. For this analysis we have taken the third generation squark mass parameters ($M_{\tilde{q}_3}, M_{\tilde{u}_3}$ and $M_{\tilde{d}_3}$) as free parameters. For \tilde{t}_1 masses within the reach of the LHC experiments at 7 TeV, this scenario is not constrained at all by the jets + \cancel{E}_T data obtained with hard cuts on kinematic variables like \cancel{E}_T and m_{eff} .

EW sector same as	S ($blj \cancel{E}_T$) (<i>Cut Set 1</i> of [20])	S ($b\tau j \cancel{E}_T$) (<i>Cut Set 1</i> of [14])
P1	426(4.8*)	82(2.0**)
P2	449(5.0)	8(0.2)
P3	309(3.4*)	313(7.5)
P4	249(2.8*)	233(5.6)
P5	456(5.1)	64(1.5)
P6	251(2.8*)	2(0.04)
P7	219(2.4*)	24(0.6)

Table 4: Number of events and the significance for $\mathcal{L} = 1 \text{ fb}^{-1}$ from pure stop-stop production using NLO cross sections from PROSPINO. Significance for each case is given in the parentheses and entries marked with * (**) indicate that the signal is observable for $1 < \mathcal{L} \leq 5 \text{ fb}^{-1}$ ($5 < \mathcal{L} \leq 10 \text{ fb}^{-1}$). For this table $m_{\tilde{t}_1}$ is 207.

We have used softer cuts proposed in [14, 20]. The $m_{\tilde{t}_1}$ mass reach via the above signals has been checked using different EW scenarios.

For the $blj \cancel{E}_T$, $l = e$ and μ , signal we have used the following cuts from [20]. We have selected events with one isolated lepton, one *tagged* b jet, at least 2 jets, $\cancel{E}_T \geq 75$ and P_T of *tagged* b jet ≤ 80 . The SM backgrounds after these cuts are available in Table 6 of [20].

For the $b\tau j \cancel{E}_T$ signal we have used the following cuts from [14] which studied this signal for the first time. We have demanded events with one *tagged* b jet, one *tagged* τ jet, no

isolated lepton, $\cancel{E}_T \geq 70$ and P_T of *tagged* τ jet ≥ 40 . SM background details after these cuts are available in Table 1 of [14].

In the light stop scenario if $\text{BR}(\tilde{\chi}^\pm \rightarrow \tilde{\tau}_1 \nu_\tau, \tilde{\nu}_\tau \tau) = 100\%$ then it is estimated that $m_{\tilde{t}_1} \leq 280$ (305) can be probed by $b\tau j \cancel{E}_T$ signal with $\mathcal{L} = 5(10)\text{fb}^{-1}$. This is similar to the $m_{\tilde{t}_1}$ reach obtained in [14] where the light EW sector was taken to be as in mSUGRA. Typical signal sizes for the benchmark points and the corresponding (S/\sqrt{B}) are presented in Table 4 for $m_{\tilde{t}_1} = 207$. The sensitivity of the signal to the EW sector is illustrated by this table.

Models with EW sectors as in P2 and P5 (with large leptonic BR of the chargino) give the maximum stop mass reach with $blj \cancel{E}_T$ signal. For these models $m_{\tilde{t}_1} \leq 275$ (305) can be probed by $blj \cancel{E}_T$ signal with $\mathcal{L} = 5(10)\text{fb}^{-1}$. Otherwise stop mass reach with $\mathcal{L} = 5(10)\text{fb}^{-1}$ varied between 230-260 (260-290) for the rest of the benchmark points.

It has been noted that the $b\tau j \cancel{E}_T$ signal will be disfavoured if $\tilde{\tau}_1$ is the NLSP and $\tilde{\tau}_1 - \tilde{\chi}_1^0$ co-annihilation is the main mechanism for relic density production. Similar degradation of the $blj \cancel{E}_T$ signal occurs if $\tilde{\chi}_1^\pm$ is the NLSP and $\tilde{\chi}_1^\pm - \tilde{\chi}_1^0$ co-annihilation contributes significantly to the relic density production. Both the signal will be degraded if \tilde{t}_1 and $\tilde{\chi}_1^\pm$ masses are close together leading to difficulties in b tagging.

We next consider the $blj \cancel{E}_T$ and the $b\tau j \cancel{E}_T$ signal in the LSG scenario discussed in the introduction following [14]. In this scenario we have treated M_3 as a free parameter in addition to the soft breaking parameters for the third generation squarks. Here all squarks except \tilde{t}_1 are assumed to be beyond the reach of the LHC 7 TeV experiments. We use different EW sectors in the unconstrained MSSM from Fig. 1.

The first information required is the lower limit on $m_{\tilde{g}}$, if any, in this scenario. As noted earlier the limits on $m_{\tilde{g}}$ in models where all squarks (including \tilde{t}_1) are assumed to be heavy and gluinos are light are changed significantly in the unconstrained MSSM. The lower limits on $m_{\tilde{g}}$ in P1, P2 and P3 are 450, 500, 620 respectively from jets + \cancel{E}_T data. One would naively expect the above limits to be valid in the LSG scenario as well since the strong cuts of ATLAS eliminates the signal from light stop pairs if any [14].

But a more stringent lower bound on $m_{\tilde{g}}$ in the LSG scenario arises from the $blj \cancel{E}_T$ signal [3]. Using 1.03fb^{-1} data the ATLAS group have excluded gluino masses below 500-520 for $m_{\tilde{t}_1}$ in the range 125 - 300. The $m_{\tilde{g}}$ limit is insensitive to $m_{\tilde{t}_1}$ since the hard ATLAS cuts eliminate the events from \tilde{t}_1 pair production.

We shall use softer cuts [14, 20] to simulate the above signals. However, we have op-

	$t\bar{t}$	QCD	$W + 1j$	$W + 2j$
σ (pb)	85.5	7.7×10^7	1.4×10^4	5.2×10^3
C1	28.728	2.2×10^5	3.1×10^3	9.53×10^2
C2	14.0519	1.07×10^4	8.2939	8.5925
C3	3.5662	1.2465×10^2	1.1499	1.9352
C4	1.8647	12.9337	0.5005	0.8375
C5	1.7219	0.0052	0.4051	0.7097

Table 5: The LO cross-sections (including efficiency) of the SM backgrounds after the cuts(C1 - C5) .

timized the cuts in [20] (see below). Our main aim is to find the stop mass reach for a fixed gluino mass consistent with the LHC data. For $blj \cancel{E}_T$ signal we have implemented the following optimized cuts in succession to enhance the signal to background ratio.

- We have selected events with one isolated lepton (C1).
- We have selected events with one *tagged b* jet (C2).
- We have demanded events with P_T of leading jet ≥ 120 (C3).
- Events with missing transverse energy (\cancel{E}_T) ≥ 70 are selected (C4).
- Events with $M_{eff} \geq 300$ are selected (C5).

The response of the SM backgrounds to these cuts are presented in Table 5. We have also studied the $b\tau j \cancel{E}_T$ signal, analysed for the first time in [14] using the cuts proposed in that paper.

For $m_{\tilde{g}} = 550$ the reach in $m_{\tilde{t}_1}$ for $\mathcal{L} = 10 \text{ fb}^{-1}$ is displayed in Table 6 for different EW scenarios. The highest stop mass can be probed in P2 with our $blj \cancel{E}_T$ signal at $\mathcal{L} = 10 \text{ fb}^{-1}$ is 375. However, the signal may also be degraded due to the degeneracies discussed in the light \tilde{t}_1 scenario. Tick marks in Table 6 indicate the channel via which the highest $m_{\tilde{t}_1}$ can be probed. It is clear that the signals are sensitive to the EW sector and the two proposed signals are complements each other.

EW sector same as	$m_{\tilde{t}_1}$ reach	Reach obtained by	
		$blj \cancel{E}_T$ signal	$b\tau j \cancel{E}_T$ signal
P1	310	✓	-
P2	375	✓	-
P3	330	-	✓
P4	325	-	✓
P5	350	✓	-
P6	335	✓	-
P7	305	✓	-

Table 6: Stop mass reach in different EW models for $m_{\tilde{g}} = 550$ for $\mathcal{L} = 10 \text{ fb}^{-1}$ in the LSG scenario using NLO cross sections. Tick mark indicates the channel for which the mass reach is obtainable.

3 Conclusions

The present lower limits on the sparticle masses in mSUGRA obtained by the current experiments at the LHC are primarily governed by the strongly interacting sparticles (the squarks and the gluinos).

However, strong limits on sparticle masses in the EW sector-much above the corresponding limits from LEP- emerge due to the correlations among these masses in mSUGRA. For example, the mass of the LSP is constrained by $m_{\tilde{\chi}_1^0} \gtrsim 160$ [40]. This constraint may have important consequences for low mass neutralino DM and the direct search for the neutralinos [13, 39, 40] and neutralino mass reconstruction [49]. The importance of light neutralino scenarios of cosmological importance has been discussed in the context of LHC experiments by [50].

Since the SUSY breaking mechanism is essentially unknown till this date it is worthwhile to revisit the above limits in an unconstrained MSSM with no correlation among the sparticle masses in the strong and EW sectors. In order to scan the parameter space we have varied the sparticle masses focusing on light EW sectors as described in section 2.1. All soft breaking masses in this sector are assumed to be below 200. Some important departures from the mSUGRA spectrum which have important consequence for neutralino DM as well as new physics search at the LHC are S1) no correlation between the chargino and the LSP mass is

assumed, S2) the left sleptons could be lighter than the right sleptons and S3) the sleptons belonging to the first two generations could be lighter or heavier than the lighter stau mass eigenstate. The present paper is, therefore, an extension of [14, 20] which for simplicity assumed the masses of the EW sparticles to be correlated as in mSUGRA. The scenario S1 can be motivated by mSUGRA type model with non-universal gaugino masses [30] while the other two scenarios by models involving non-universal scalar masses [31, 32].

We then vary the parameters in the EW sector and delineate the parameter space consistent with the WMAP data on DM relic density (see Fig. 1). As a consequence of S1) neutralinos with mass $\gtrsim 35$ are found to be consistent with WMAP data as long as the LSP is bino dominated or is a mixture of bino and wino. This revives the possibility of neutralino annihilation via a nearly on shell Z boson and/or lighter h-boson. Moreover a chargino NLSP is a distinct possibility in this scenario and chargino-neutralino co annihilation is a viable DM producing mechanism as is readily seen from Fig 1. In S2 with relatively light L-type sleptons and sneutrino, neutralino annihilation can proceed efficiently. Moreover, LSP - sneutrino co annihilation may become an important DM producing mechanism for each LSP mass. This mechanism is especially important for S3 when $\tilde{\tau}_1$ is relatively heavy. None of these mechanisms are viable in mSUGRA in view of the LHC data.

Using the ATLAS selection criteria [2] we find that in an unconstrained MSSM, the limits on the squarks and gluinos derived in mSUGRA changes either way by at most 10-12% for most choices of the light EW sector consistent with the WMAP data as described in Fig. 1 (sub-section 2.3). This shows that i) the limits on $m_{\tilde{q}}$ and $m_{\tilde{g}}$ derived in mSUGRA are approximately valid in the unconstrained MSSM and ii) EW sparticles much lighter than that in mSUGRA are consistent with the LHC data. If the leptonic BR of chargino decays are much larger than that in mSUGRA, then the lepton veto in the ATLAS selection procedure relaxes the gluino mass limits appreciably. This is illustrated by the points P2 and P6 which belongs to the scenario S2. It may be recalled that a similar relaxation was noted in the context of old Tevatron experiments (see the 1st paper of [33]). For very heavy squarks, the gluino mass limit L4 (see sub-section 2.3) reduces by 20 % . This is the largest relaxation in $m_{\tilde{g}}$ noted by us and is illustrated by the point P1 belonging to scenario S1. It is, therefore, fair to conclude that the current LHC data in the jets + \cancel{E}_T channel is by and large insensitive to the choice of the EW sector and EW sparticles having masses just above the corresponding LEP limits are very much allowed.

In the absence of a suitable $e^+ - e^-$ collider it is not easy to directly test the EW sector even if the sparticles in this sector are light. The simulations of the LHC 14 TeV experiments [18] suggest that the clean tri-lepton signal from chargino-neutralino production or the dilepton + \cancel{E}_T signal stemming from light slepton pair production may not be viable at the experiments at 7 TeV.

We have, therefore, considered two scenarios each with a subset of the strongly interacting sparticles and a light EW sector within the reach of the LHC, They are i) the light stop scenario and ii) the light stop gluino (LSG) scenario. In both cases we consider $blj \cancel{E}_T$ [3, 14] and $b\tau j \cancel{E}_T$ [20] signal. We also follow the selection criteria suggested in these references.

In the light stop scenario we find that if the lighter chargino decays into τ rich final states with large BR (see, e.g., points P3 and P4 in Table 2) $m_{\tilde{t}_1}$ upto 260 (305) can be probed by the $b\tau j \cancel{E}_T$ signal, investigated for the first time in [14], for $\mathcal{L} = 5$ (10) fb^{-1} . On the other hand if $\tilde{\chi}^\pm$ decays into e or μ with large BR (see, e.g., P2 and P5) $m_{\tilde{t}_1}$ upto 275 (305) can be probed by the $blj \cancel{E}_T$ signal for $\mathcal{L} = 5$ (10) fb^{-1} . For the rest of the benchmark points the mass reach varies between 230 - 260 (260 - 290) for $\mathcal{L} = 5$ (10) fb^{-1} . It was noted in [14, 20] that the signal size is quite sensitive to the EW sector. This is also reflected by Table 6. It should, however, be borne in mind that the above signals can be degraded due to some unexpected degeneracies in the spectrum as discussed in sub-section 2.3.

Signal of the LSG scenario in the $blj \cancel{E}_T$ channel has also been considered by the ATLAS collaboration. However, as pointed out in [14, 20] they use very hard cuts which practically eliminate the signal from \tilde{t}_1 pair production. As a result the gluino mass reach obtained by them is practically insensitive to $m_{\tilde{t}_1}$. Using softer cuts following [14, 20] we find the reach in $m_{\tilde{t}_1}$ for a fixed $m_{\tilde{g}} = 550$ and display the results in Table 6. The signal size indeed shows some sensitivity to the EW sector. Of course the signal will be degraded if the degeneracies as discussed above are present. We conclude by noting that supersymmetry with a light electroweak sector consistent with the WMAP and LEP constraints is very much allowed by the current LHC data.

References

- [1] For reviews on Supersymmetry, see, *e.g.*, H. P. Nilles, Phys. Rep. **110**, 1 (1984); H. E. Haber and G. Kane, Phys. Rep. **117**, 75 (1985); J. Wess and J. Bagger, *Supersymmetry*

and Supergravity, 2nd ed., (Princeton University Press, Princeton, 1991); M. Drees, P. Roy and R. M. Godbole, *Theory and Phenomenology of Sparticles*, (World Scientific, Singapore, 2005).

- [2] ATLAS Collaboration, arXiv:1109.6572 [hep-ex].
- [3] ATLAS Collaboration, ATLAS-CONF-2011-130 (2011).
- [4] ATLAS Collaboration, Phys. Rev. D **85**, 012006 (2012); ATLAS Collaboration, Phys. Lett. B **709**, 137 (2012).
- [5] CMS Collaboration, Phys. Rev. Lett. **107**, 221804 (2011); Report No. CMS-PAS-SUS-11-010; Report No. CMS-PAS-SUS-11-010; Report No. CMS-PAS-SUS-11-015.
- [6] D. Feldman, Z. Liu and P. Nath, Phys. Rev. D **81**, 095009 (2010); H. Baer, S. Kraml, A. Lessa and S. Sekmen, J. High Energy Phys. **02**, 055 (2010); H. K. Dreiner, M. Kramer, J. M. Lindert and B. O’Leary, J. High Energy Phys. **04**, 109 (2010); H. Baer, V. Barger, A. Lessa, and X. Tata, J. High Energy Phys. **06**, 102 (2010); N. Bhattacharyya, A. Datta and S. Poddar, Phys. Rev. D **82**, 035003 (2010); B. Altunkaynak, M. Holmes, P. Nath, B. D. Nelson and G. Peim, Phys. Rev. D **82**, 115001 (2010); B. Mukhopadhyaya and S. Mukhopadhyay, Phys. Rev. D **82**, 031501 (2010); S. Akula *et al*, Phys. Lett. B **699**, 377 (2011); N. Chen, D. Feldman, Z. Liu, P. Nath and G. Peim, Phys. Rev. D **83**, 035005 (2011); P. Bechtle *et al*, arXiv:1105.5398; M. Guchait and D. Sengupta, Phys. Rev. D **84**, 055010 (2011); O. Buchmueller *et al*, arXiv: 1110.3568; M. Badziak and K. Sakurai, arXiv:1112.4796 [hep-ph].
- [7] A. H. Chamseddine, R. Arnowitt and P. Nath, Phys. Rev. Lett. **49**, 970 (1982); R. Barbieri, S. Ferrara and C. A. Savoy, Phys. Lett. B **119**, 343 (1982); L. J. Hall, J. Lykken and S. Weinberg, Phys. Rev. D **27**, 2359 (1983); P. Nath, R. Arnowitt and A. H. Chamseddine, Nucl. Phys. B **227**, 121 (1983); N. Ohta, Prog. Theor. Phys. **70**, 542 (1983).
- [8] For the latest limits on the sparticle masses from LEP experiments: see, e.g., <http://lepsusy.web.cern.ch/lepsusy/>.

- [9] W. L. Freedman and M. S. Turner, *Rev. Mod. Phys.* **75**, 1433 (2003); L. Roszkowski, *Pramana* **62**, 389 (2004). G. Bertone, D. Hooper and J. Silk, *Phys. Rept.* **405**, 279 (2005);
- [10] H. Baer and X. Tata in *Physics at the Large Hadron Collider*, Indian National Science Academy, A Platinum Jubilee Special Issue (Eds. Amitava Datta, B. Mukhopadhyaya and A. Raychaudhuri; Springer, 2009).
- [11] E. Komatsu *et al*, (WMAP Collaboration), *Astrophys. J. Suppl.* **192**, 18 (2011).
- [12] N. Baro, F. Boudjema and A. Semenov, *Phys. Lett. B* **660**, 550 (2008).
- [13] S. Akula, D. Feldman, Z. Liu, P. Nath and G. Peim, *Mod. Phys. Lett. A* **26**, 1521 (2011).
- [14] Nabanita Bhattacharyya, Arghya Choudhury and Amitava Datta, *Phys. Rev. D* **84**, 095006 (2011).
- [15] C. Boehm, A. Djouadi and M. Drees, *Phys. Rev. D* **62**, 035012 (2000); J. R. Ellis, K. A. Olive and Y. Santoso, *Astropart. Phys.* **18**, 395 (2003).
- [16] H. Baer, K. Hagiwara and X. Tata, *Phys. Rev. D* **35**, 1598 (1987); R. Arnowitt and P. Nath, *Mod. Phys. Lett. A* **2**, 331 (1987); H. Baer and X. Tata, *Phys. Rev. D* **47**, 2739 (1993); H. Baer, C. Kao and X. Tata, *Phys. Rev. D* **48**, 5175 (1993); S. Mrenna, G. Kane, G. D. Kribs and J. D. Wells, *Phys. Rev. D* **53**, 1168 (1996); Zack Sullivan, Edmond L. Berger, *Phys. Rev. D* **78**, 034030 (2008).
- [17] For recent discussions on slepton pair production at hadron colliders and references to earlier works see: G. Bozzi, B. Fucks and M. Klasen, *Phys. Rev. D* **74**, 015001 (2006); *Nucl. Phys. B* **777**, 157 (2007); *Nucl. Phys. B* **794**, 46 (2008); F. Borzumati and K. Hagiwara, *J. High Energy Phys.* **1103**, 103 (2011).
- [18] See, e.g., Fig. **13.5** in CMS physics Technical Design Report, Vol-II (Eds. A. De Roeck *et al*), *J. Phys. G* **34**, 995 (2007).
- [19] N. Bhattacharyya and Amitava Datta, *Phys. Rev. D* **80**, 055016 (2009).

- [20] Nabanita Bhattacharyya, Arghya Choudhury and Amitava Datta, Phys. Rev. D **83**, 115025 (2011).
- [21] N. Bhattacharyya, A. Datta, M. Maity, Phys. Lett. B **669**, 316 (2008).
- [22] C. Brust, A. Katz, S. Lawrence and R. Sundrum, arXiv:1110.6670 [hep-ph].
- [23] N. Desai and B. Mukhopadhyaya, arXiv:1111.2830 [hep-ph].
- [24] K. Huitu, J. Laamanen, L. Leinonen, Phys. Rev. D **84**, 075021 (2011).
- [25] X. J. Bi, Q. S. Yan and P. F. Yin, arXiv: 1111.2250 [hep-ph].
- [26] S. Bornhauser, M. Drees, S. Grab and J. S. Kim Phys. Rev. D **83**, 035008 (2011); M. Drees, M. Hanussek and J. S. Kim, arXiv: 1201.5714.
- [27] B. He, T. Li and Q. Shafi, arXiv:1112.4461 [hep-ph].
- [28] C. Boehm, A. Djouadi and Y. Mambrini, Phys. Rev. D **61**, 095006 (2000).
- [29] S. P. Das, A. Datta and M. Guchait, Phys. Rev. D **65**, 095006 (2002); S. P. Das, A. Datta and M. Maity, Phys. Lett. B **596**, 293 (2004).
- [30] R. Arnowitt, A. H. Chamseddine and P. Nath, Problems in Unification and Supergravity, La Jolla Institute (1983) (see <http://www.osti.gov/bridge/servlets/purl/5986323-fY7neR/5986323.pdf>); J. R. Ellis, K. Enqvist, D. V. Nanopoulos and K. Tamvakis, Phys. Lett. B **155**, 381 (1985); M. Drees, Phys. Lett. B **158**, 409 (1985); A. Corsetti and P. Nath, Phys. Rev. D **64**, 125010 (2001); S. P. Martin, Phys. Rev. D **79**, 095019 (2009).
- [31] P. Moxhay and K. Yamamoto, Nucl.Phys.B 256, 130 (1985); B. Gato, Nucl.Phys.B 278, 189 (1986); N. Polonsky and A. Pomarol Phys. Rev. D **51**, 6532 (1995); J. Ellis, D.V. Nanopoulos and K. A. Olive, Phys. Lett. B **525**, 308 (2002).
- [32] M. Drees, Phys. Lett. B **181**, 279 (1986); Y. Kawamura, H. Murayama and M. Yamaguchi, Phys. Rev. D **51**, 1337 (1995).
- [33] Amitava Datta, M. Guchait and N. Parua, Phys. Lett. B **395**, 54 (1997); Amitava Datta, Aseshkrishna Datta, M. K. Parida, Phys. Lett. B **431**, 347 (1998); Amitava Datta, Aseshkrishna Datta, M. Drees and D. P. Roy, Phys. Rev. D **61**, 055003 (2000);

- [34] S. Heinemeyer, W. Hollik and G. Weiglein, Phys. Rep. **425**, 265 (2006); S. Heinemeyer, Int. J. Mod. Phys. A **21**, 2659 (2006); G. Degrassi *et al*, Eur. Phys. J. C **28** (2003) 133; S. Heinemeyer, W. Hollik and G. Weiglein, Eur. Phys. J. C **9** (1999) 343.
- [35] ALEPH, DELPHI, L3 and OPAL Collaborations, The LEP Working Group for Higgs Boson Searches, Phys. Lett. B **565**, 61 (2003)
- [36] G. Belanger *et al*, Comp. Phys. Comm. **182**, 842 (2011).
- [37] A. Djouadi, J. L. Kneur and G. Moultaka, Comp. Phys. Comm. **176**, 426 (2007).
- [38] M. Muhlleitner, A. Djouadi and Y. Mambrini, Comp. Phys. Comm. **168**, 46 (2005).
- [39] E. Aprile *et al* (XENON100 Collaboration), Phys. Rev. Lett. **107**, 131302 (2011); Phys. Rev. D **84**, 061101 (2011); Astropart. Phys. **35** (2012), 573-590.
- [40] C. Beskidt, W. de Boer, D. I. Kazakov and F. Ratnikov, arXiv:1202.3366 [hep-ph].
- [41] ATLAS Collaboration, arXiv:1202.1408 [hep-ex]; arXiv:1202.1414 [hep-ex]; arXiv:1202.1415 [hep-ex].
- [42] CMS Collaboration, arXiv:1202.1416[hep-ex]; arXiv:1202.1487[hep-ex]; arXiv:1202.1488 [hep-ex]; arXiv:1202.1489 [hep-ex]; arXiv:1202.1997 [hep-ex].
- [43] S. Heinemeyer, O. Stal and G. Weiglein, arXiv:1112.3026 [hep-ph]; A. Arbey, M. Battaglia, A. Djouadi, F. Mahmoudi and J. Quevillon, Phys. Lett. B **708**, 162 (2012); A. Djouadi, O. Lebedev, Y. Mambrini and J. Quevillon, arXiv:1112.3299 [hep-ph]; O. Buchmueller *et al*, arXiv:1112.3564 [hep-ph]; S. Akula, B. Altunkaynak, D. Feldman, P. Nath and G. Peim, arXiv:1112.3645 [hep-ph]; S. Heinemeyer, arXiv:1202.1991 [hep-ph]; K. A. Olive, arXiv:1202.2324 [hep-ph]; J. Ellis and K. A. Olive, arXiv:1202.3262 [hep-ph].
- [44] See, *e.g.*, A. Pukhov, CalcHEP—a package for evaluation of Feynman diagrams and integration over multi-particle phase space (hep-ph/9908288). For the more recent versions see: <http://www.ifh.de/pukhov/calchep.html>.
- [45] T. Sjostrand, P. Eden, C. Friberg, L. Lonnblad, G. Miu, S. Mrenna and E. Norrbin, Comp. Phys. Comm. **135**, 238 (2001); For a more recent version see, J. High Energy Phys. **0605**, 026 (2006).

- [46] H. L. Lai *et al.* [CTEQ Collaboration], Eur. Phys. J. C **12**, 375 (2000); P. M. Nadolsky *et al.* [CTEQ Collaboration], Phys. Rev. D **78**, 013004 (2008). See also, <http://www.phys.psu.edu/cteq>.
- [47] M. Mangano *et al.* , J. High Energy Phys. **0307**, 001 (003).
- [48] W. Beenakker, R. Hoepker and M.Spira, arXiv: hep-ph/9611232.
- [49] M. Drees and C-L.Shan, J. Cosmol. Astropart. Phys. 06, 011 (2007); O.Mena, S. Palomarez-Ruiz and S. Pascoli,Phys. Lett. B **664**, 92 (2008); A. M. Green,J. Cosmol. Astropart. Phys., 0807,005 (2008); C-L. Shan, New.J.Phys.11,105013(2009); N. Bernal, A. Goudelis, Y. Mambrini and C. Munoz,J. Cosmol. Astropart. Phys. 0901,046(2009). J. Billard, F. Mayetand and D. Santos,Phys. Rev. D **83**, 075002 (2011).
- [50] S. Choi, S. Scopel, N. Fornengo and A. Bottino, Phys. Rev. D **85**, 035009 (2012).